IOP Publishing Superconductor Science and Technology
Supercond. Sci. Technol. 31 (2018) 085004 (7pp) https://doi.org/10.1088/1361-6668/aac943

Internal strain induced superconductivity in arc melted $Ti_{0.97}Fe_{0.03}$ alloy

L S Sharath Chandra[1], M K Chattopadhyay[1,2], Jagdish Chandra[1], M A Manekar[1], S K Pandey[3], R Venkatesh[4] and S B Roy[1,2]

[1] Magnetic and Superconducting Materials Section, Raja Ramanna Center for Advanced Technology, Indore, Madhya Pradesh-452 013, India
[2] Homi Bhabha National Institute, Training School Complex, Anushakti Nagar, Mumbai 400 094, India
[3] School of Engineering, Indian Institute of Technology Mandi, Kamand, Himachal Pradesh-175005, India
[4] Low Temperature Laboratory, UGC-DAE Consortium for Scientific Research, Madhya Pradesh-452 017, India

E-mail: lsschandra@rrcat.gov.in

Received 20 February 2018, revised 28 May 2018
Accepted for publication 31 May 2018
Published 25 June 2018

Abstract

Alloys with a small amount of iron dissolved in α-titanium are known to have superconducting transition temperatures (T_C) up to ~3.5 K which are higher than that expected from the density of states. The origin of this enhancement still remains unanswered in spite of extensive theoretical and experimental studies. We show here with the help of x-ray diffraction, metallography, resistivity and heat capacity measurements as well as the calculation of density of states that the internal strain developed during rapid cooling of the sample from the high temperature β-phase is responsible for the anomalous high value of $T_C = 3.3$ K in the arc melted $Ti_{0.97}Fe_{0.03}$ alloy. The relaxation of the lattice by expelling a large amount of iron from the α-phase in the equilibrium state lowers the T_C below 2.4 K when the $Ti_{0.97}Fe_{0.03}$ sample is annealed inside the α-phase. These results indicate that the superconductivity in $Ti_{1-x}Fe_x$ alloys is mostly confined to the α-phase.

Keywords: Ti-Fe alloys, superconductivity, structural properties

(Some figures may appear in colour only in the online journal)

1. Introduction

In the late 1950s Matthias *et al* [1, 2] had shown for the first time that the superconducting transition temperature T_C was increased when titanium and zirconium were alloyed with the magnetic transition elements such as Fe, Mn, Co and Cr. The T_Cs of $Ti_{1-x}TM_x$ (TM = Fe, Co, Mn and Cr) alloys were found to be in the range 3.5–4.5 K for $x = 0.1$ which were an order of magnitude higher than the $T_C = 0.2$–0.5 K [3] in elemental Ti. This increase in T_C was higher than that expected for an enhancement in the density of states when these magnetic elements are added [1]. This was contradictory to the understanding prevailing at that time. This result was interpreted in terms of superconductivity mediated by magnetic interactions [4, 5], which is now extensively used to explain the superconducting properties in the recently discovered Fe based high temperature pnictide superconductors [6].

The subsequent studies on the $Ti_{1-x}TM_x$ alloys by Hake *et al* [7], Cape [8], Strongin *et al* [9] and Raub *et al* [10], however, negated the possibility of magnetic interaction mediated superconductivity. These studies also revealed the lack of a magnetic moment on iron in the dilute $Ti_{1-x}Fe_x$ alloys. On the basis of a broad resistive transition and a composition independent critical current density, Hake *et al* suggested that the superconductivity in the $Ti_{1-x}TM_x$ alloys was of a filamentary type [7]. Cape [8] observed that the $Ti_{1-x}Mn_x$ ($x \leqslant 0.03$) alloys were not superconducting when quenched after annealing at 1000 °C, whereas the alloys were superconducting with a T_C up to 3.2 K when quenched after annealing at 690 °C. From the metallography studies on the $Ti_{1-x}Mn_x$ alloys, Cape [8] concluded that the precipitation of the body centred cubic (bcc) β-Ti-TM phase was responsible for the superconductivity in $Ti_{1-x}TM_x$ alloys [8]. On the other hand, Raub *et al* [10] observed that only arc melted $Ti_{1-x}Fe_x$ samples were superconducting with a T_C of 3.2 K. The

martensitic hexagonal close packed (hcp) α-phase forms with a β-phase precipitation [11] when the $Ti_{1-x}Fe_x$ alloys are quenched after annealing in the β-phase at 930 °C for 2 h. De Souza *et al* [11] reported that the micro-structure of α-phase at room temperature was dependent on the cooling rate when quenched after annealing in the β-phase, however, it was independent of the cooling rate when quenched after annealing in the α-phase [11]. Their studies revealed that the amount of β-phase precipitation is inversely proportional to the cooling rate [11]. These results are contradictory to the conclusions drawn in the earlier studies [8]. Even in the single phase α-$Ti_{1-x}Fe_x$ alloys, the superconducting volume fraction was only about 30% of the sample at T_C [12]. Later, other possibilities such as Coulomb and exchange interactions between conduction electrons and impurity states [13], and a dynamical Jahn–Teller effect [14] have been put forward to explain the anomalous superconducting properties of the $Ti_{1-x}Fe_x$ alloys. However, these models could not account for the effect of annealing on the T_C [15]. Prekul *et al* [16] suggested the presence of spin fluctuations in $Ti_{1-x}Fe_x$ alloys from the measurement of resistivity. Collings argued [15] on the basis of studies by Prekul *et al* [16] and Hake *et al* [7], that the suppression of the jump in heat capacity at T_C was related to the presence of spin fluctuations. However, such a suppression of the jump at T_C is not observed in the $Ti_{1-x}V_x$ alloys where the spin fluctuations are considerable [17, 18]. From the comparison of metallographic studies with the calorimetric data, Ho and Collings [19] found a correlation between the dependence of T_C on the annealing conditions in the $Ti_{0.925}Fe_{0.075}$ alloy with the amount of ω-phase present in the sample. Although this study proved that the T_C reduces when ω-phase forms, it does not explain why T_C is higher in the as-cast samples. Moreover, the T_C was dependent on the annealing conditions even in the single phase α-$Ti_{1-x}Fe_x$ alloys in the composition range where the ω-phase does not form [10]. Therefore, it is not clear why there is a variation of T_C in the α-$Ti_{1-x}Fe_x$ alloys when the annealing conditions are changed.

Here we present a detailed study of the structural, electrical and thermodynamic properties of α-$Ti_{0.97}Fe_{0.03}$ alloy subjected to various thermal treatments. We show that the internal strain generated during rapid cooling of the sample from the high temperature β-phase induces superconductivity in the Ti rich $Ti_{1-x}Fe_x$ alloys at temperatures higher than that expected for a change in the density of states when Fe is alloyed with Ti.

2. Experimental and computational details

The $Ti_{0.97}Fe_{0.03}$ sample was prepared by melting the constituent elements (99.95+% purity) in an arc-furnace under 99.999% pure Ar atmosphere. The sample was flipped and re-melted six times to improve the homogeneity. X-ray diffraction (XRD) measurements were performed on the angle dispersive XRD beamline BL-12 using 15 keV (0.8×10^{-10} m) x-rays from the INDUS-2 synchrotron radiation source, a six circle diffractometer (Huber 5020) and a scintillation point detector in the step scan mode [20]. The wave-length was accurately calibrated using the XRD pattern of Si powder (NIST standard). The temperature dependence of the resistivity and heat capacity of this $Ti_{0.97}Fe_{0.03}$ sample were measured in a Physical Property Measurement System (Quantum Design, USA). Scanning electron microscopy (SEM) images were taken using NoVa NanoSEM 450 instrument (FEI Company, USA) operated at 18 kV. Compositional analysis was done using an X-Flash 6130 energy dispersive spectroscopy (EDS) attachment (Bruker, Germany) and Esprit software.

Electronic structure calculations for α-Ti and α-$Ti_{0.97}Fe_{0.03}$ alloy for the nonmagnetic state were carried out using the state-of-the-art full potential linearized augmented plane-wave method [21]. The muffin-tin sphere radius was chosen to be 2.7 Bohr. Local density approximation was used for the exchange-correlation functional [22]. A mesh size of (10,10,10)k-points was used for the calculations. Self-consistency was achieved by demanding the root mean square change in the effective potential to be smaller than 10^{-6}. The density of states was calculated using a 400k-point mesh in the Brillouin zone.

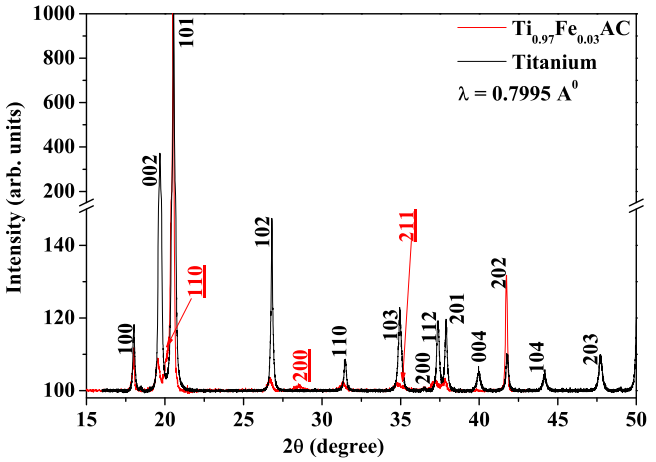

Figure 1. X-ray diffraction patterns of titanium and $Ti_{0.97}Fe_{0.03}AC$ samples. Substitution of iron in titanium results in the precipitation of the β-phase in the hcp matrix. Weak reflections corresponding to the bcc phase are also seen.

3. Results and discussion

Figure 1 shows the comparison of the XRD pattern of an as-cast $Ti_{0.97}Fe_{0.03}$ sample (we call this sample $Ti_{0.97}Fe_{0.03}AC$) with that of elemental titanium. The $Ti_{0.97}Fe_{0.03}AC$ sample has predominantly formed in the hcp structure of α-titanium. However, peaks corresponding to the (110), (200) and (211) reflections of the β-phase are also visible with small intensity. The approximate fraction of the β-phase in the $Ti_{0.97}Fe_{0.03}AC$ sample is estimated (by integrating the diffraction peaks) to be about 6.6%. The lattice parameters of the hcp phase are found to be $a = 2.973(1)$ Å and $c = 4.751(2)$ Å for $Ti_{0.97}Fe_{0.03}AC$ and $a = 2.969(3)$ Å and $c = 4.713(4)$ Å for α-titanium. The lattice parameter of bcc phase in $Ti_{0.97}Fe_{0.03}AC$ is 3.261(4) Å.

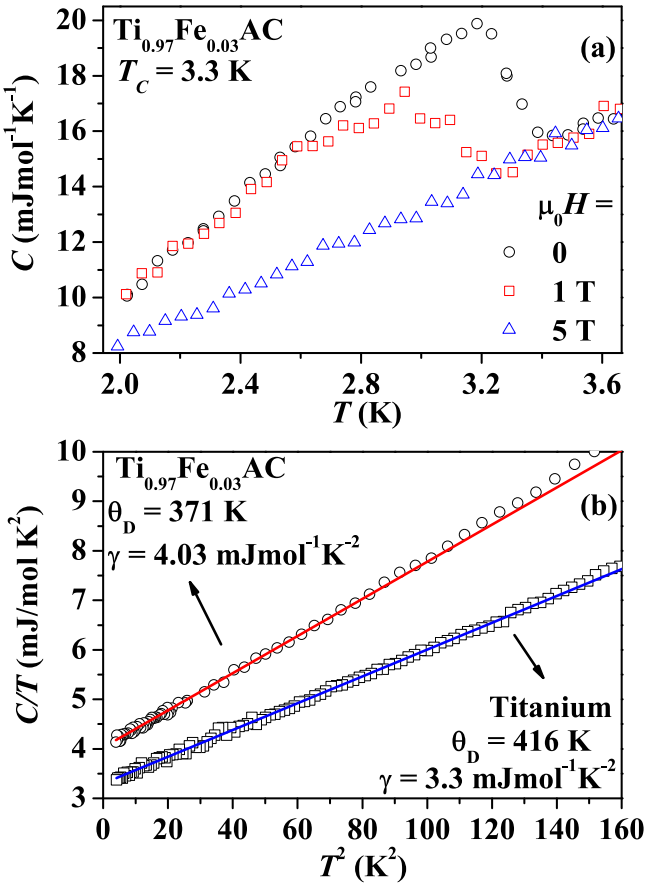

Figure 2. (a) Temperature dependence of heat capacity of $Ti_{0.97}Fe_{0.03}AC$ sample below 3.6 K in various applied magnetic fields. (b) Temperature dependence of heat capacity plotted as C/T versus T^2 for titanium and $Ti_{0.97}Fe_{0.03}AC$ samples in zero and 5 T magnetic fields respectively. Open symbols are the experimental data points and the solid lines represent the linear fit to the experimental data.

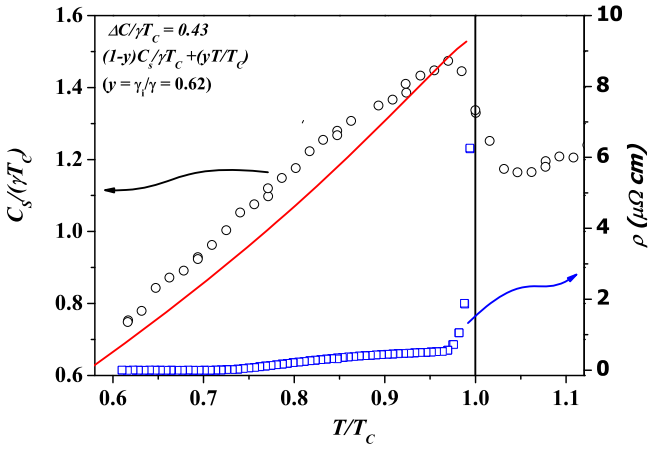

Figure 3. Temperature variation of $C_S/\gamma T_C$ and resistivity in zero magnetic field across the transition. Open symbols are the experimental data points and the solid lines are fits to the experimental data (see text).

Figure 2(a) shows the temperature dependence of the heat capacity $C(T)$ of the $Ti_{0.97}Fe_{0.03}AC$ sample in zero magnetic field. A jump in $C(T)$ below 3.4 K is an indication of superconductivity in the bulk of the sample. The $T_C = (3.3 \pm 0.1)$ K is estimated as that temperature at which the temperature derivative of $C(T)$ in zero magnetic field shows a minimum. The superconductivity is suppressed to a temperature below 2 K with the application of a magnetic field of 5 T. The value of T_C for the $Ti_{1-x}Fe_x$ alloys shows a spread from 1.5 to 3.7 K depending upon the way the sample is prepared [15].

Figure 2(b) shows the $C(T)$ plotted as C/T versus T^2 for titanium and $Ti_{0.97}Fe_{0.03}AC$ samples in zero and 5 T magnetic fields respectively. The $C(T)$ below ≈10 K can be expressed as $C(T) = \gamma T + \beta T^3$, where γ is the Sommerfeld coefficient of electronic heat capacity and β is related to the Debye temperature as $\theta_D = (1\,943.66/\beta)^{1/3}$. The γ and θ_D estimated by a linear fit (solid lines) to the experimental data (open symbols) of $Ti_{0.97}Fe_{0.03}AC$ alloy are (4.03 ± 0.01) mJ mol^{-1} K^{-2} and (371 ± 2) K, respectively. Similarly, γ and θ_D for titanium are (3.30 ± 0.01) mJ mol^{-1} K^{-2} and (416 ± 1) K, respectively. The values of γ and θ_D for titanium are in agreement with those reported in literature for a 99.98% purity Ti sample [23].

Figure 3 shows the plot of $C_S/\gamma T_C$ as well as the resistivity (both in zero magnetic field) as a function of T/T_C, where C_S is the electronic part of the heat capacity in the superconducting state. The open symbols are the experimental data points. The jump in heat capacity at T_C expressed as $\Delta C/\gamma T_C$ is about 0.43. This value is at least three times lower than the Bardeen–Cooper–Schrieffer (BCS) value of 1.43 [24]. Such a deviation indicates that either a small fraction of the sample is superconducting or the nature of the superconductivity is unconventional [24]. The temperature dependence of resistivity $\rho(T)$ of this sample across the transition plotted in figure 3 shows a sharp drop when the sample is cooled below 3.4 K. Zero resistance is observed only below 2.4 K. This indicates that there is a distribution of T_Cs over a large temperature range. Cape argued that the superconductivity in $Ti_{1-x}Fe_x$ alloys is due to the β-phase precipitation [8]. The amount of β-phase is only about 6% in the $Ti_{0.97}Fe_{0.03}AC$ sample. However, the jump in the heat capacity suggests that at least 30% of the sample is superconducting. Therefore, the superconductivity in the present sample is not due to a filamentary bcc β-phase alone, rather the superconductivity lies mostly in the α-phase.

The heat capacity of a sample which is partly superconducting can be expressed as $[C_S/\gamma T_C] = (1-y)[C_S/\gamma T_C]_{BCS} + yT/T_C$, where $[C_S/\gamma T_C]_{BCS}$ is the heat capacity of the BCS superconductor [25–27] and $y = \gamma_i/\gamma$ is the fraction of the sample that is not superconducting. The parameter y is varied so as to get a $[C_S/\gamma T_C]$ curve whose jump at T_C matches with the experimental value of 0.43. The red solid line in figure 3 is the curve for $y = 0.62$, which indicates that at about 38% of the sample is superconducting at T_C and the rest of the sample (62%) remains in the normal state with a finite electrical resistance and a finite Sommerfeld coefficient γ_i.

The curve does not match the experimental $[C_S/\gamma T_C]$ at any temperature below T_C. The theoretical curve lies below the experimental data, which again supports the assumption

that there is a distribution of T_Cs over a large temperature range. Therefore, increasing fractions of the sample volume become superconducting when the temperature is decreased below $T_C = 3.3$ K.

The metallic radius of titanium is 147 pm whereas that of iron is 126 pm. Therefore, the lattice parameters of the α-phase of $Ti_{1-x}Fe_x$ alloys should in principle be less than those of elemental Ti. Experimentally, both the lattice parameters a and c of α-phase in the $Ti_{0.97}Fe_{0.03}$AC sample are found to be larger than those of α-Ti. This indicates that the $Ti_{0.97}Fe_{0.03}$AC sample is highly strained. Brandt and Ginzburg [28] observed that the increase of T_C in a 99.99% α-titanium single crystal is little when 10 kbar of hydrostatic pressure is applied [28]. However, the plastic deformation changed the T_C irreversibly to a value which is higher than that of the sample kept under hydrostatic pressure [28]. Baskin *et al* [29] have shown that the T_C of titanium in ω-phase increases from 2 K at 40 kbar to about 3.4 K at 55 kbar. After decompression, the ω-phase was retained in titanium at normal pressure [30], however, the sample was not superconducting [31]. Ponosov *et al* [32] have shown from a study of the temperature dependence of Raman spectra, the presence of ω-phase precipitates in α-titanium below 100 K at ambient pressure. On the other hand, Ho and Collings have suggested that the enhancement of T_C in mechanically deformed Ti-Mo alloys is due to the modifications in the phonon dispersion spectrum [33]. Hence, we believe that the enhanced T_C of $Ti_{0.97}Fe_{0.03}$AC sample is due to the internal strain developed by the disorder resulting from the rapid cooling of the sample during the preparation.

In order to understand the origin of enhanced T_C in the as-cast sample, we have subjected a $Ti_{0.97}Fe_{0.03}$AC sample to two annealing schedules, (1) 850 °C for 2 h and then quenched into ice (we call this sample $Ti_{0.97}Fe_{0.03}$AN1) and (2) 800 °C for 48 h and then cooled to room temperature at a rate of 2 °C h^{-1} (we call this sample $Ti_{0.97}Fe_{0.03}$AN2). The $Ti_{0.97}Fe_{0.03}$ alloy undergoes a β to α transition at about 850 °C when the sample is cooled from the β-phase. Figure 4 shows the XRD pattern of $Ti_{0.97}Fe_{0.03}$AN2 alloy at room temperature. The sample is almost single phase with an α-titanium structure, and it is not possible to detect the presence of any secondary bcc phase. The positions of peaks corresponding to the possible bcc phase are marked with a $*$ where the background appears to be higher than normal indicating that if present, the bcc phase will be only in traces. The lattice parameters of the $Ti_{0.97}Fe_{0.03}$AN2 alloy are $a = 2.955\,7(7)$ Å and $c = 4.719(2)$ Å. These values are similar to those of elemental titanium indicating that a considerable amount of strain has been relieved after annealing followed by slow cooling.

The inset to figure 4 shows the comparison of $C(T)/T$ versus T^2 in 5 T magnetic fields for $Ti_{0.97}Fe_{0.03}$AC and $Ti_{0.97}Fe_{0.03}$AN2. The values of $\gamma = (3.43 \pm 0.01)$ mJ mol^{-1} K^{-2} and $\theta_D = (427 \pm 2)$ K of $Ti_{0.97}Fe_{0.03}$AN2 are comparable to those of elemental titanium rather than those of $Ti_{0.97}Fe_{0.03}$AC This indicates that the variation of the internal strain due to the thermal treatments influence the electron–phonon interaction in the $Ti_{1-x}Fe_x$ alloys. The density of states of α-Ti and α-$Ti_{0.97}Fe_{0.03}$AC

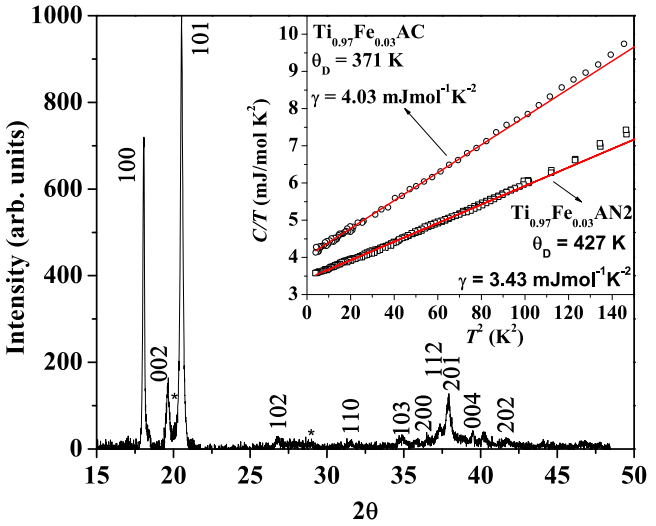

Figure 4. X-ray diffraction pattern of $Ti_{0.97}Fe_{0.03}$ alloy after annealing at 800 °C for 48 h followed by cooling to the room temperature at a rate of 2 °C h^{-1}. (Inset) Temperature dependence of heat capacity plotted as C/T versus T^2. Open symbols are the experimental data points and the red solid lines represent the straight line fit to the data.

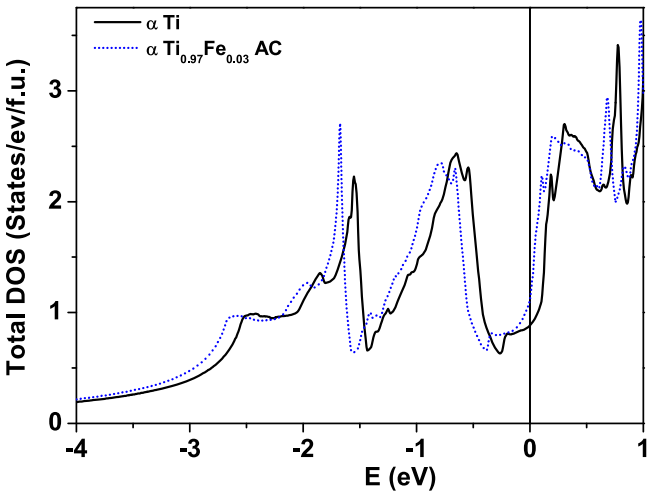

Figure 5. Density of states of α-Ti, and as-cast α-$Ti_{0.97}Fe_{0.03}$ samples.

calculated in the rigid band approximation are shown in figure 5. We have taken the experimental lattice parameters as the input parameters for the calculation. The density of states of α-Ti (black solid line) reported here is similar to that reported in the literature [34]. The calculation of density of states for the Fe substituted sample is carried out by adding excess valence electrons to the Ti lattice, which is equivalent to the Fe addition. The Fermi level of α-Ti lies in the valley. When Fe is added into Ti, the additional electrons fills up the band and the Fermi level shifts away from the valley. The strength of the electron–phonon interaction can be gauged by estimating the electron–phonon coupling constant (λ_{ep}) as $\lambda_{ep} = (\gamma/\gamma_0) - 1$ where γ_0 is the Sommerfeld coefficient of electronic specific heat obtained from the band structure calculations [35]. The γ_0 for α-Ti is about 2.08 mJ mol^{-1} K^{-2}. Therefore, λ_{ep} of α-Ti and $Ti_{0.97}Fe_{0.03}$AC are about 0.58 and 0.53 respectively. However,

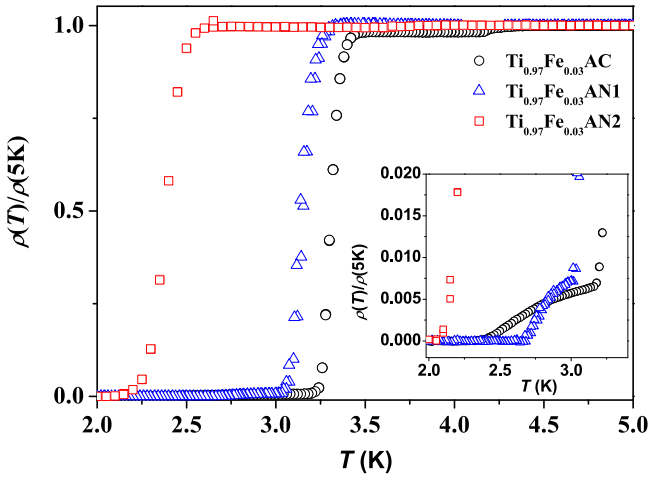

Figure 6. Temperature dependence of the resistivity across T_C in $Ti_{0.97}Fe_{0.03}AC$, $Ti_{0.97}Fe_{0.03}AN1$ and $Ti_{0.97}Fe_{0.03}AN2$. (Inset) Expanded view of the resistivity-temperature curves below 3.3 K.

the effective electron–phonon interaction that is responsible for the superconductivity may be weak due to the existence of other interactions such as spin fluctuations [36]. The effective electron–phonon coupling constant that is responsible for superconductivity can be estimated from the T_C, and θ_D using the McMillan formula [37], as long as λ_{ep} does not exceed unity. The λ_{ep} thus estimated for α-Ti, $Ti_{0.97}Fe_{0.03}AC$ samples are 0.38 and 0.53 respectively. This indicates that the stretched lattice of $Ti_{0.97}Fe_{0.03}AC$ is favourable for the electron–phonon interaction to become effective to induce superconductivity below 3.4 K.

Figure 6 shows the effect of annealing on the superconductivity in $Ti_{0.97}Fe_{0.03}$ alloy. Here, we compare the temperature dependence of resistivity $\rho(T)$ plotted as $\rho(T)/\rho(5\,K)$ versus T across the T_C for the $Ti_{0.97}Fe_{0.03}AC$, $Ti_{0.97}Fe_{0.03}AN1$ and $Ti_{0.97}Fe_{0.03}AN2$ samples. The $Ti_{0.97}Fe_{0.03}AC$ alloy show a sharp drop in resistivity when cooled below 3.4 K. However, as shown in the inset, $\rho(T)$ does not go to zero just below 3.4 K, but at 2.4 K. The T_C of $Ti_{0.97}Fe_{0.03}AN1$ decreases slightly, but the behaviour remains same as that of $Ti_{0.97}Fe_{0.03}AC$. In $Ti_{0.97}Fe_{0.03}AN2$ sample, a sharp transition is observed at $T_C = 2.3$ K.

Figure 7 shows the metallography images (1000×) of $Ti_{0.97}Fe_{0.03}$ alloy subjected to different thermal treatments. Figure 7(a) shows that the $Ti_{0.97}Fe_{0.03}AC$ sample has thin needle like structures with a width of about 1 μm or less. This is the case for the alloys that are quenched from a temperature above the $\alpha - \beta$ transition temperature of about 850 °C. The grain size increases when the sample is annealed at temperatures below the $\alpha - \beta$ transition temperature. Figure 7(b) shows the image for the $Ti_{0.97}Fe_{0.03}AN1$ sample. Now the grains are bigger by an order of magnitude as compared to the $Ti_{0.97}Fe_{0.03}AC$ sample. The grain size is more than 100 μm when slow cooled (2 °C h^{-1}) after annealing at 800 °C for 48 h (figure 7(c)). This growth eliminates most of the strain. We have performed SEM and EDS measurements in order to get quantitative information on composition of our samples. Figure 8 shows the high resolution SEM images of (a) the

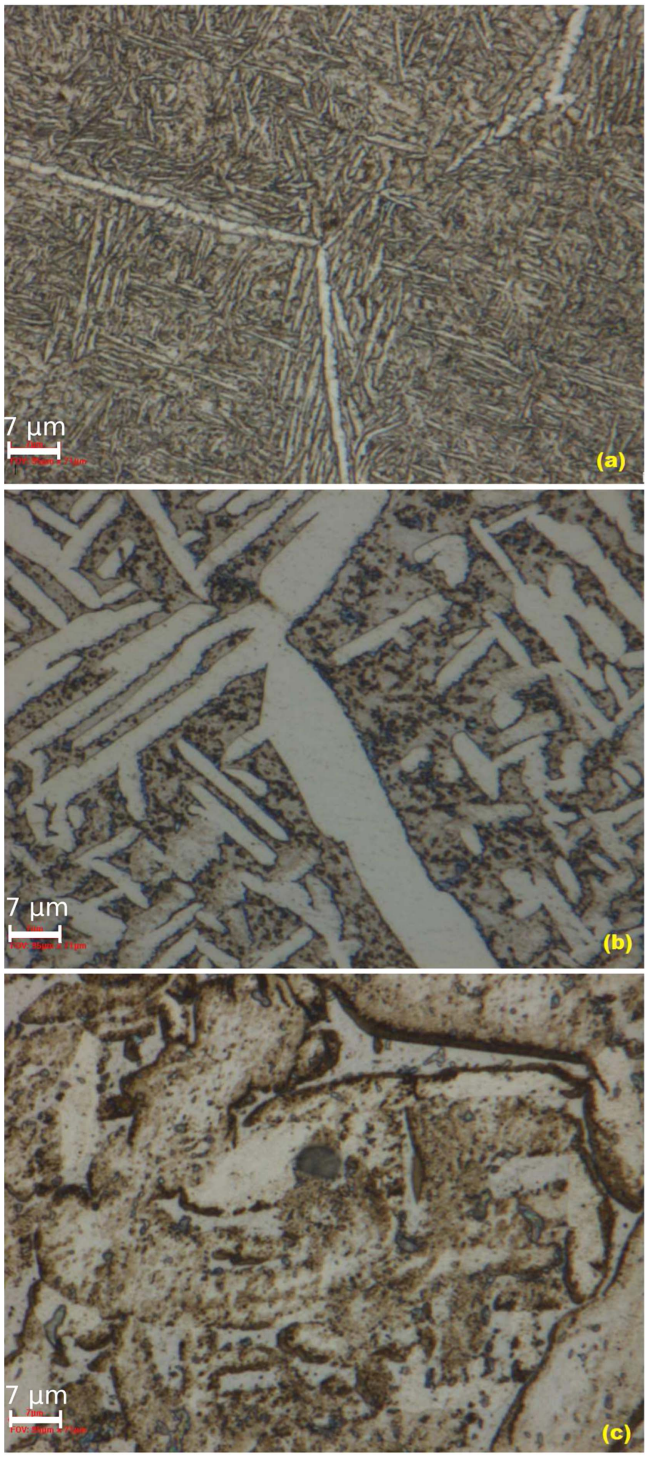

Figure 7. 1000× optical metallography images of $Ti_{0.97}Fe_{0.03}$ alloy (a) as-cast (b) annealed at 850 °C and then ice quenched (c) annealed at 800 °C for 48 h and then cooled to room temperature with the rate of 2 °C h^{-1}.

$Ti_{0.97}Fe_{0.03}AC$ and (b) the $Ti_{0.97}Fe_{0.03}AN2$ samples. The $Ti_{0.97}Fe_{0.03}AC$ sample shows a lamellar structure. We have performed the EDS measurements at eight different positions on this sample. The composition is uniform with (97.5 ± 0.6) at% of titanium and (2.5 ± 0.6) at% of iron. This indicates that the sample is predominantly α-phase. The amount of β-phase present in the sample, when Ti alloys with β stabilizers are

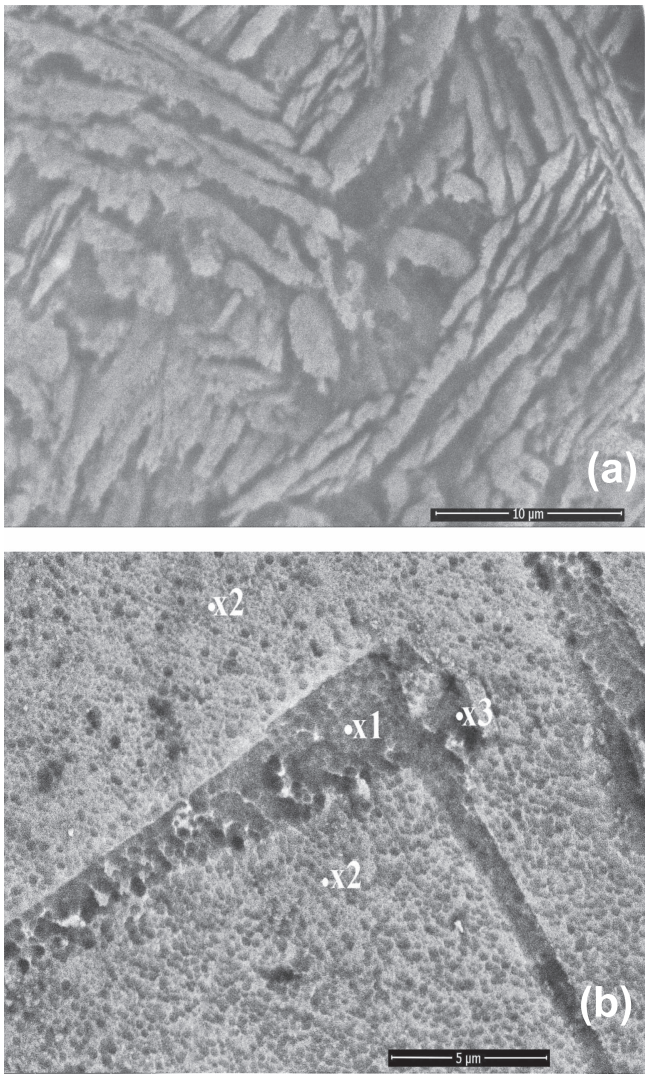

Figure 8. High resolution SEM images of (a) $Ti_{0.97}Fe_{0.03}AC$ and (b)$Ti_{0.97}Fe_{0.03}AN2$ samples. The marked places are some of the many points where the EDS has been carried out.

cooled from the liquid depends strongly on the cooling rate [38]. The β-phase does not precipitate when the cooling rate is higher than 18 K s^{-1}. The quantity of α-phase decreases and the amount of β-phase increases when the cooling rate is decreased. Since, $Ti_{0.97}Fe_{0.03}AC$ is arc melted, the cooling rate of the sample from the melt to the α-phase region is very high and uncontrolled. Hence, the amount of β-phase ;in the $Ti_{0.97}Fe_{0.03}AC$ sample is low [38] and the size of the β-phase precipitates in such alloys will be less than 50 nm [39]. Therefore, the dark and light regions observed in $Ti_{0.97}Fe_{0.03}AC$ sample probably correspond to different orientations of the α-phase. The morphology of $Ti_{0.97}Fe_{0.03}AN2$ sample is different from the $Ti_{0.97}Fe_{0.03}AC$ sample. We can identify three kinds of micro-structure in the $Ti_{0.97}Fe_{0.03}AN2$ sample. Large grains with sub-grains of size 200–300 nm form the major part of the sample (marked as x2). The composition in this area of the sample is mainly titanium with less than 0.5 at% of iron. The area marked x1 contains about 3 at% of iron in titanium whereas very few isolated places (marked as x3) were seen with rich iron content of up to 10 at%. It is reported in literature that the solubility limit of iron in titanium in the equilibrium state is less than a percent [10]. Therefore, the titanium expells the iron from the α-phase region when Ti rich Ti-Fe alloys are annealed. Therefore, the presence of 3 at% of iron in the α-phase of $Ti_{0.97}Fe_{0.03}AC$ sample leads to a strained α-phase lattice. These results indicate that the superconductivity is mostly confined to the α-phase of the $Ti_{0.97}Fe_{0.03}$ alloys.

4. Conclusion

We have investigated the $Ti_{0.97}Fe_{0.03}$ alloy subjected to various thermal treatments. The arc melted sample (as-cast) shows needle type micro-structure, and a T_C of 3.3 K, whereas the sample that is annealed at 800 °C for 48 h and then cooled to room temperature at a rate of 2 °C h^{-1} shows millimetre sized grains and a T_C of 2.4 K. The analysis of the XRD patterns of elemental titanium and the $Ti_{0.97}Fe_{0.03}$ alloy subjected to various thermal treatments show that the lattice is stretched when iron is added to titanium and the stretching is due to disorder induced during the rapid cooling of the sample. These results indicate that the enhancement of T_C in the as-cast $Ti_{0.97}Fe_{0.03}$ alloy is governed by the internal stress present in the α-phase of the sample and the superconductivity is mostly confined to the α-phase of the $Ti_{1-x}Fe_x$ alloys.

Acknowledgments

We thank Archna Sagdeo and A K Sinha for their help in x-ray diffraction measurements, Vishal Dhamgaye for his help in obtaining optical images and Anirudha Bose for helpful discussion on metallography of Ti alloys.

ORCID iDs

L S Sharath Chandra https://orcid.org/0000-0002-1253-6035

References

[1] Matthias B, Compton V B, Suhl H and Corenzwit E 1959 Ferromagnetic solutes in superconductors *Phys. Rev.* **115** 1597–8
[2] Matthias B and Corenzwit E 1955 Superconductivity of zirconium alloys *Phys. Rev.* **100** 626–7
[3] Steele M C and Hein R A 1953 Superconductivity of titanium *Phys. Rev.* **92** 243–7
[4] Akhiezer A I and Pomeranchuk I Y 1959 Interaction between conduction electrons in ferromagnets *Sov. Phys.-JETP* **9** 605–7
Akhiezer A I and Pomeranchuk I Y 1959 *Zh. Eksp. Teor. Fiz.* **36** 859–62

[5] Bardeen J and Schrieffer J R 1961 Recent developments in superconductivity *Progress in Low Temperature Physics* vol 3 (Amsterdam: Elsevier) ch 6 pp 170–287

[6] Fernandes R M and Chubukov A V 2017 Low-energy microscopic models for iron-based superconductors: a review *Rep. Prog. Phys.* **80** 014503 and references therein

[7] Hake K K, Leslie D H and Berlincourt T G 1962 Low temperature resistivity minima and negative magnetoresistivities in some dilute superconducting Ti alloys *Phys. Rev.* **127** 170–9

[8] Cape J A 1963 Superconductivity and localized magnetic states in Ti-TM alloys *Phys. Rev.* **132** 1486–92

[9] Strongin M, Maxwell E and Reed T B 1964 Ac susceptibility measurements on transition metal superconductors containing rare earth and ferromagnetic metal solutes *Rev. Mod. Phys.* **36** 164–8

[10] Raub E, Raub C H J, Roschel E, Compton V B, Geballe T H and Matthias B T 1967 The α-Ti-Fe solid solution and its superconducting properties *J. Less-Common Met.* **12** 36–40

[11] De Souza S J, Quesne C, Servant C and Severac C 1985 The influence of iron and thermal treatments on the microstructure of commercially pure titanium *Metallography* **18** 353–65

[12] Heiniger F and Muller J 1964 Bulk superconductivity in dilute hexagonal titanium alloys *Phys Rev.* **134A** 1407–9

[13] Ganguly B N, Upadhyaya U N and Sinha K P 1966 Indirect interaction involving impurity states in superconductors *Phys. Rev.* **146** 317–21

[14] Kumar N 1970 Attractive electron–electron interaction induced by the dynamical Jahn-Teller effect involving degenerate impurity orbitals: a theory of the impurity enhancement of the superconductive transition temperature in dilute alloys *Phys. Rev.* B **2** 2500–11

[15] Collings E W 1983 *A Source Book of Titanium Alloy Superconductivity* (New York: Plenum)

[16] Prekul A F, Shcherbakov A S and Volkenshtein N V 1976 The resistivity and the anomalous superconducting transitions in $Ti_{1-x}Fe_x$ alloys ($0 \leqslant x \leqslant 0.2$) *Fiz. Nizk. Temp.* **2** 1399–404

[17] Matin M, Sharath Chandra L S, Meena R K, Chattopadhyay M K, Sinha A K, Singh M N and Roy S B 2014 Spin-fluctuations in $Ti_{0.6}V_{0.4}$ alloy and its influence on the superconductivity *Physica* B **436** 20–5

[18] Matin M, Sharath Chandra L S, Pandey S K, Chattopadhyay M K and Roy S B 2014 The influence of electron–phonon coupling and spin fluctuations on the superconductivity of the Ti-V alloys *Eur. Phys. J.* B **87** 131-10

[19] Ho J C and Collings E W 1973 Calorimetric studies of superconductive proximity effects in a two-phase Ti-Fe (7.5%) alloy *Proc. Int. Conf. Low Temp. Phys.* **3** 403–7

[20] Sinha A K, Sagdeo A, Gupta P, Kumar A, Singh M N, Gupta R K, Kane S R and Deb S K 2011 Commissioning of angle dispersive x-ray diffraction beamline on Indus-2 *AIP Conf. Proc.* **1349** 503–4

[21] The Elk FP-LAPW Code http://elk.sourceforge.net

[22] Perdew J P and Wang Y 1992 Accurate and simple analytic representation of the electron-gas correlation energy *Phys. Rev.* B **45** 13244–9

[23] Kneip G D Jr, Betterton J O Jr and Scarbrough J O 1963 Low temperature specific heats of titanium, zirconium and hafnium *Phys. Rev.* **130** 1687–92

[24] Poole C P Jr., Farach H A, Creswick R J and Prozorov R 2007 *Superconductivity* 2nd edn (Amsterdam: Academic)

[25] Sharath Chandra L S, Chattopadhyay M K, Roy S B and Pandy S K 2016 Thermal properties and electronic structure of superconducting germanide skutterudites and : a multi-band perspective *Phil. Mag.* **96** 2161–75

[26] Shyam S, Sharath C L S, Chattopadhyay M K and Roy S B 2015 Evidence of multiband superconductivity in the β-phase $Mo_{1-x}Re_x$ alloys *J. Phys.: Condens. Matter* **27** 045701

[27] Padamsee H, Neighbor J E and Shiffman C A 1973 Quasiparticle phenomenology for thermodynamics of strong-coupling superconductors *J. Low Temp. Phys.* **12** 387–411

[28] Brandt N B and Ginzburg N I 1965 Investigation of the effects of hydrostatic pressure and plastic deformation on the superconducting properties of titanium *J. Exp. Theor. Phys.* **49** 1706–14
Brandt N B and Ginzburg N I 1966 *Sovt. Phys.-JETP* **22** 1167–71

[29] Bashkin I O, Tissen V G, Nefedova M V and Ponyatovsky E G 2007 Superconducting temperature of the ω-phase in Ti, Zr, and Hf metals at high pressures *Physica* C **453** 12–4

[30] Dewaele A, Stutzmann V, Bouchet J, Bottin F, Occelli F and Mezouar M 2015 High pressure-temperature phase diagram and equation state of titanium *Phys. Rev.* B **91** 134108

[31] Degtyareva V F, Karimov Yu S and Rabinkin A G 1973 Superconductivity and magnetic susceptibility of the α and ω modifications of titanium and zirconium *Fiz. Tverd. Tela* **15** 3436–8

[32] Ponosov Yu S, Streltsov S V and Syassen K 2012 Optical phonon self energies in titanium phases: effect of electron-phonon interaction *High Press. Res.* **32** 138–44

[33] Ho J C and Collings E W 1971 Enhancement of the superconducting transition temperatures of Ti-Mo (5.7 at%) alloys by mechanical deformation *J. Appl. Phys.* **42** 5144–50

[34] Bakonyi I, Ebert H and Liechtenstein A I 1993 Electronic structure and magnetic susceptibility of the different structural modifications of Ti, Zr and Hf metals *Phys. Rev.* B **48** 7841–9

[35] Tari A 2003 *The Specific Heat of Mater at Low Temperature* (London: Imperial College Press)

[36] Bose S K 2008 Electron-phonon coupling and spin fluctuations in 3d and 4d transition metals: implications for superconductivity and its pressure dependence *J. Phys.: Condens. Matter* **21** 025602

[37] McMillan W L 1968 Transition temperature of strong-coupled superconductors *Phys. Rev.* **167** 331–44

[38] Filip R, Kubiak K, Ziaja W and Sieniawski 2003 The effect of microstructure on the mechanical properties of two-phase titanium alloys *J. Mater. Process. Technol.* **133** 84–9

[39] Markovskya P E and Semiatinb S L 2011 Tailoring of microstructure and mechanical properties of Ti-6Al-4V with local rapid (induction) heat treatment *Mater. Sci. Eng.* A **528** 3079–89